



Title: MOTION OF FLOATING WIND TURBINES	Delivered:
	Availability: Unclassified
Student: Børge Linde	Number of pages: 45

Abstract:

Motion of floating wind turbines has been studied. A literature study on different concepts and what tools are available for simulating them is presented. Marintek's simulation software SIMO is used for time simulations. In the calculations, the hydrodynamic forces, mooring line forces and aerodynamic forces from the tower and rotor are taken into account. In addition a pitch control algorithm is used for the rotor blades. Results are compared to available experimental results from model tests. The structure studied is a 5 MW version of the Hywind concept.

Keyword:

Floating Wind Turbine. SIMO. Hywind.

Advisor:

Professor Bjørnar Pettersen

Address:
NTNU
Department of Marine Technology
N-7491 Trondheim

Location
Marinteknisk Senter
O. Niensens vei 10

Tel. +47 73 595501
Fax +47 73 595697

Preface

A literature study of different concepts and what tools are available for simulating them was chosen as a starting point. In a previous project thesis I studied the motion of a free floating cylinder in waves, as a background for this master thesis.

Marintek's simulation software SIMO is used for time simulations of a 5 MW version of the floating wind turbine Hywind. Results from SIMO are compared to available results from a previous model test of the concept.

An essential part of this master thesis has been to learn how to use the SIMO software. A lot of time was spent on this and on the extension needed to include a wind turbine in the simulations.

Uncertainties about how the model test version actually was built have caused some problems. A deviance in the geometry input I had access to was found late in the semester and a lot of work was done twice. As a consequence the result presentation is a bit shorter than what was planned.

Acknowledgements

This work has been carried out under supervision of Professor Bjørnar Pettersen at the Department of Marine Technology, the Norwegian University of Science and Technology. I am grateful for his input and for the opportunity to work with this subject.

I am also grateful to all the people who contributed during this thesis work:

- Marintek: for giving me permission to internal information regarding the implementation of a wind turbine module to SIMO. Especially Petter Andreas Berthelsen for helping me start the project. And also Knut Mo, Gro Baarholm, Ivar Fylling and Halvor Lie for additional help and information.

- Statoil: for kindly giving me access to results from experimental model tests. Especially Rune Yttervik for giving detailed information about the model tests.

Finally I would like to thank my parents, Leif K. Linde and Anne Elise Linde, for all their support throughout my studies.

Børge Linde

July 2010

Nomenclature

General

- Symbols and abbreviations will in general be explained as they are given in the text. Some of the standard symbols listed underneath will however not be repeated.
- Subscripts i generally denotes direction in generalized force direction i . Here $i=1,2,3$ denotes x-, y- and z-direction respectively and $i=4,5,6$ denotes the moment components about the same axis. These i directions (or degrees of freedom) are denoted: 1=Surge, 2=Sway, 3=Heave, 4=Roll, 5=Pitch, 6=Yaw. In addition subscript i will be used for describing element no. i in a distributed element model used in SIMO.

Roman symbols

A_{ij}	Added mass matrix element ij
B_{ij}	Damping matrix element ij
C_{ij}	Restoring force matrix element ij
B_{linear}	Linear damping matrix
$B_{quadratic}$	Quadratic damping matrix
D	Diameter of buoy or element in strip model
D_{WP}	Diameter of buoy at the water plane
R	Radius of buoy
z_G	Vertical center of gravity (VCG)
Z_B	Vertical center of buoyancy (VCB)
A	Area of buoy cross section
A_{WP}	Cross section area at waterline
f_i	Drag force on element no. i
g	Acceleration of gravity
V	Submerged volume of the buoy
$C_{D,i}$	Non-dimensional drag coefficient for element no. i
ΔZ_i	Height of element no. i in a strip model
$C_{q,i}$	Quadratic drag coefficient for element no. i , given in full dimensions
$U_{rel,i}$	Relative velocity of element no. i in a local element coordinate system
v_i	Water particle velocity in a local element coordinate system
\dot{X}_i	Velocity of element no. i
U_i	Current flow velocity in local element coordinate system

Greek symbols

Π	The constant 3.14159....
ρ	Mass density of fluid
η_i	Motion response of buoy in DOF i
γ	Gamma. Peakedness parameter

Abbreviations

FOWT	Floating Offshore Wind Turbine
DNV	Det Norske Veritas
RAO	Response Amplitude Operator (linear transfer-function)
VCG	Vertical center of gravity
VCB	Vertical center of buoyancy
GM_T	Transverse metacentric height
DOF	Degrees of freedom
2D	Two-dimensional
3D	Three-dimensional
BEM	Blade Element Momentum
OC3	Offshore Code Comparison Collaboration
LF	Low Frequency
WF	Wave frequency
FFT	Fast Fourier Transform
NREL	National Renewable Energy Laboratory
KC	Kaulegan-Carpenter number
Re	Reynolds number
k/D	Roughness number
Hs	Significant wave height
Tp	Peak period

Table of contents

Preface	I
Acknowledgements	II
Nomenclature	III
List of tables:	VII
List of figures:	VII
1 INTRODUCTION	8
1.1 Background and motivation.....	8
1.2 Outline of the thesis	9
2 LITERATURE STUDY - Floating Offshore Wind Turbines and what tools are available for simulating them	10
2.1 General methods for testing offshore structures.....	10
2.2 Numerical tools available for simulating FOWT	10
2.2.1 Offshore Code Comparison Collaboration (OC3).....	10
2.2.2 Marintek software - SIMO	11
2.3 Different FOWT concepts	13
2.3.1 Hywind	13
2.3.2 SWAY	14
2.3.3 Njord.....	14
2.3.4 WindSea	15
2.3.5 WindFloat.....	16
2.4 Previous work	16
2.4.1 Basic study on spar-buoys.....	17
3 NUMERICAL MODEL.....	18
3.1 Learning SIMO.....	19
3.2 Model specifications - uncertainties	20
3.3 Linear and quadratic potential forces	21

3.3.1	Implementation in SIMO	22
3.4	Damping	24
3.4.1	Quadratic drag forces	25
3.5	Restoring forces and moments	26
3.5.1	Linear stiffness matrix.....	26
3.5.2	Mooring lines	27
3.6	Mass properties/matrix	29
3.7	Modeling the rotor module	29
3.7.1	Rotor.....	29
3.7.2	Tower	30
3.7.3	Nacelle.....	30
4	COMPARISON OF NUMERICAL MODEL WITH EXPERIMENTAL MODEL TEST RESULTS.....	31
4.1	The different test conditions	31
4.2	Comparison procedure.....	31
4.3	Test number 1,2 and 3 – without wind	34
4.3.1	Possible improvements.....	36
4.4	Test number 4, 5 and 6 – including wind	37
5	CONCLUSION.....	41
6	RECOMMENDATIONS FOR FURTHER WORK.....	42
7	REFERENCES	43
APPENDIX A – Calculation of mass and stiffness properties. (not published)		

List of tables:

Table 2.1 – Overview of OC3 participants.....	11
Table 3.1 – Main particulars of the 5 MW version of the Hywind concept.....	18
Table 4.1 – Specification of test conditions	31
Table 4.2 - Comparison of some results from test condition 1, 2 and 3. Drag forces evaluated up to mean surface.....	35
Table 4.3 - Comparison of some results from test condition 1, 2 and 3. Drag forces evaluated up to instantaneous surface.	37
Table 4.4 - Comparison of some results from test condition 4, 5 and 6. Drag forces evaluated up to mean surface.....	39

List of figures:

Figure 2.1 – Hywind full-scale prototype	13
Figure 2.2 – Illustration photo of the Sway concept	14
Figure 2.3 – Illustration photo of the Njord concept.....	15
Figure 2.4 – Illustration photo of the WindSea concept	15
Figure 2.5 – Illustration photo of the WindFloat concept	16
Figure 3.1 – Illustration photo of the Hywind concept	18
Figure 3.2 – Picture from the experimental model-scale test set-up.....	19
Figure 3.3 – Hydrodynamic-wave-excitation force in heave as calculated from Wadam	23
Figure 3.4 – Illustration photo from the numerical simulations.....	28

1 INTRODUCTION

1.1 Background and motivation

It is known that oil and gas reservoirs will run empty in the future. Still the world is in growth and demands more energy than ever. In a time of environmental change and where the planet's health is in focus we see a growing demand for clean energy.

A well known renewable energy source is the wind, and traditional windmills have been installed on land for many years. Wind turbines have also been successfully installed at relatively shallow water depths. This has typically been done by piled cylinders or gravity-based foundations. Typical water depth is 2-30 meters. In September 2009 the Norwegian based company NorWind successfully installed six jacket foundations for offshore wind at Alpha Ventus, Germany's first offshore wind farm (norwind.no 2009). The foundations are installed on an average of 30 meters depth. Most of the offshore wind farms in operation today are located off the coasts of Great Britain and Denmark, but at present time these kinds of farms are showing up all over the world. Both Statoil and Statkraft are involved in the development of the 315 MW Sheringham Shoal offshore wind farm in United Kingdom (UK) (Statoil.com 2009). True Forewind they are also involved in the UK offshore wind farm project at the Doggerbank field. The target installed capacity is set to 9 GW. (Statoil.com 2008)

It is of interest to move the wind energy production to even deeper waters. Vast resources would then become available. Many floating concepts have been proposed for this purpose. In order to evaluate these concepts some new numerical codes have been developed and some existing codes have been modified for the specific purpose of analyzing offshore wind turbines. In order to see that numerical calculations are consistent with reality it is of interest to compare them to experimental test results.

1.2 Outline of the thesis

Basic theory is in general not described in this thesis, but reference is made to textbooks. Some principles will also be given in the text.

Chapter 2 presents a brief literature study on available tools for simulation of Floating Offshore Wind Turbines (FOWT). Some promising FOWT concepts will also be mentioned.

Chapter 3 presents different parts regarding how the numerical model is established in SIMO.

Chapter 4 presents a selection of results obtained from the numerical model. These are compared to available results from experimental model-scale tests.

2 LITERATURE STUDY - Floating Offshore Wind Turbines and what tools are available for simulating them

2.1 General methods for testing offshore structures

In order to investigate the behavior of offshore structures there are three main categories: numerical calculations, experimental model-scale testing and full-scale prototype testing.

Normally both numerical calculations and model testing are done before building the full scale structure. Full scale prototype testing is usually not done before the project is finalized.

2.2 Numerical tools available for simulating FOWT

Tools for simulating onshore wind turbines have been available for some time. This is also the case for offshore floating structures. In the case of floating wind turbines it is of interest to simulate the wind turbine and the floater in a coupled analysis. Several numerical codes are available for this purpose today. The status on these numerical codes is studied and some general information is given in the following text. Also learning how to use one of these numerical codes has been a major part of this thesis work. A numerical analysis of a floating wind turbine will be presented later in this report.

2.2.1 Offshore Code Comparison Collaboration (OC3)

Most of the aero-hydro-servo-elastic codes that have been developed for modeling the dynamic response of offshore wind turbines are tested within the OC3 – Offshore Code Comparison Collaboration. This is a project with code-to-code verification between the different participants. Defined tasks are analyzed by all the codes participating in the project and the results are compared. In this way all participants get indications about whether their numerical codes are consistent with similar codes, or about possible room for improvement. At an early stage this sharing of knowledge is considered to be beneficial, even though the different codes could be considered as competitors. (Jonkman 2010)

The numerical codes are quite advanced as they are so-called aero-hydro-servo-elastic codes. This means that the most advanced codes account for aerodynamics on rotor, nacelle and tower. It accounts for the regulating system of the rotor. It accounts for hydrodynamics of the

floater and for mooring. And it accounts for structural elasticity in the different material components of the system. I will not go into detail about all the different codes. Main information about participating codes and the theory applied are listed in Table 2.1. This information is found in Jonkman et al. (2010). More details about OC3 can also be found at (www.ieawind.org).

FAST	Bladed	ADAMS	HAWC2	BHawC	3Dfloat	Simo	DeepC	SESAM
Code Developer / OC3 Participant								
NREL	GH	MSC + NREL / NREL + ForWind	Rise-DTU	Siemens	UMB	Marintek	DNV / NTNU	DNV / Acciona
Aerodynamics								
(BEM or GDW) + DS	(BEM or GDW) + DS	(BEM or GDW) + DS	(BEM or GDW) + DS	(BEM or GDW) + DS	(BEM or GDW) + DS	BEM	None	None
Hydrodynamics								
Airy* + ME, Airy + PF	(Airy* or Stream) + ME	Airy* + ME, Airy + PF	Airy + ME	Airy + ME	Airy + ME	Airy + PF	Airy* + ME, Airy + PF	Airy* + ME, Airy + PF
Control System (Servo)								
DLL, UD, SM	DLL	DLL, UD	DLL, UD, SM	DLL, UD	DLL, UD	None	None	None
Structural Dynamics (Elastic)								
Turbine: FEM* + (Modal / MBS), Mooring: QSCE	Turbine: FEM* + (Modal / MBS), Mooring: UDFD	Turbine: MBS, Mooring: QSCE	Turbine: MBS / FEM, Mooring: UDFD	Turbine: MBS / FEM, Mooring: UDFD	Turbine: FEM, Mooring: FEM	Turbine: MBS, Mooring: QSCE	Turbine: MBS, Mooring: FEM	Turbine: MBS, Mooring: QSCE
Airy* – Airy wave theory +) with free surface corrections BEM – blade-element / momentum DLL – external dynamic link library DNV – Det Norsk Veritas DS – dynamic stall			GDW – generalized dynamic wake FEM* – finite-element method P) for mode preprocessing only MBS – multibody-dynamics formulation ME – Morison's equation MSC – MSC Software Corporation			PF – linear potential flow with radiation & diffraction QSCE – quasi-static catenary equations SM – interface to Simulink® with MATLAB® UD – implementation through user-defined subroutine available UDFD – implementation through user-defined force- displacement relationships		

Table 2.1 – Overview of OC3 participants

It is seen that most codes use a Blade Element Momentum (BEM) method to calculate the wind forces on the rotor blades. A general description about the state-of-the-art in design tools for FOWT and the use of BEM can be found in Cordle (2010). To simplify, it can be mentioned that BEM from aerodynamics use a similar approach as the Morison equation known from hydrodynamics. Simple BEM theory does not deal with the unsteady nature of the aerodynamics experienced by a wind turbine rotor. To account for this several corrections can be applied to the BEM model.

2.2.2 Marintek software - SIMO

In this thesis I will use the SIMO software from Marintek. I will use a rigid-body model and a BEM code for the wind turbine. It should be mentioned that Marintek also have a system where material flexibility is accounted for. This is done by combining their two codes SIMO

and RIFLEX. The version of the software I have used in this thesis is described in Sintef (2009). As the information is considered confidential I will refer to this report for details. However an overview is available at Fylling (2010) where he describes the following:

2.2.2.1 General description

SIMO is a general-purpose program for simulating motions of arbitrarily shaped floating structures, including interconnected multi-body systems. The force model comprises:

- Hydrodynamic forces: Linear and quadratic potential forces, hydrodynamic coupling effects, Morison-type force models, lumped and distributed on slender elements.
- Wind forces: Drag force due to gusty wind.
- Mechanical forces: Mooring line forces, a range of body-to-body coupling force models, control forces (DP system), and variable mass.
- Inertia- and gravity forces.
- User specified arbitrary “External Force”.

(Fylling 2010)

2.2.2.2 Floating Wind Turbine Simulation: Rigid-body Simulation by use of SIMO with Extension

A wind turbine module has been implemented in a multi-body simulation model in SIMO, see Fylling (2010). The implementation of aerodynamic rotor forces is explained:

- The blade element momentum method (BEM) is used for calculation of rotor blade element forces, a 6-component vector, is used as external load on a rotating body (Rotor).
- The Rotor is coupled to the support structure (support) by means of two radial bearings and one thrust bearing. The torque generated by the power take-off system is transferred directly from the Rotor to the Support.
- The applied BEM code will give correct time series results for rotor and blade loads under conditions of changing blade pitch angle, wind speed and direction, and tower motion.

The implementation allows more than one rotor on the same floating structure. No modification to the modeling or analysis features in SIMO has been done as part of this development. (ibid.)

2.3 Different FOWT concepts

Practically all known classes of floaters have been proposed for use as a wind turbine platform. In addition to the technical challenges it is also important to lower the cost regarding production, installation and maintenance. Some of the most promising concepts so far are briefly described here.

2.3.1 Hywind

Statoil have proposed a long draft spar-type FOWT called Hywind. It is attached to the seabed by a three-point mooring spread. An up-wind rotor is used. Extensive numerical modeling and experimental model-scale testing have been performed. Statoil have also been able to build and install a full-scale prototype of the concept. Hywind is the world's first full-scale floating wind turbine. Tests will be performed over a two-year period. A picture of the full-scale prototype is shown in Figure 2.1. (Statoil.com 2009)



Figure 2.1 – Hywind full-scale prototype

2.3.2 SWAY

The SWAY system is also a concept from a Norwegian based company, Sway AS. The tower is filled with ballast and has its center of gravity located far below the center of buoyancy. This is said to give the tower sufficient stability to resist the large loads produced by the wind turbine mounted on top of it, see (sway.no). Contrary to most wind turbine concepts the SWAY system uses a downwind rotor. The floating tower is anchored to the seabed with a single pipe and a suction anchor. The anchor tension leg is fixed to the tower by a yaw mechanism which allows the entire windmill, including the tower, to rotate with the wind direction. Extensive numerical calculations have been performed and also experimental model-scale tests. An illustration of the floater with tension leg is shown in Figure 2.2. The company has also developed their own design for a 10 MW turbine on top of the floater. The first full-scale windmill is expected to be built and installed during the period 2010 to 2012 (Statoil.com).



Figure 2.2 – Illustration photo of the Sway concept

2.3.3 Njord

The Njord concept is also from Norway. The floater looks similar to the Hywind spar-buoy, except that the draft is much less. It has mooring lines connected at different vertical levels on the structure. It basically aims to lead the horizontal forces from the tower down to the sea bottom. By this mooring design the idea is to reduce the amount of steel needed for the structure (Nilsen 2010). One of the people behind the project is also the developer behind the

numerical code 3DFloat. Both numerical simulations and experimental model-scale testing have been performed on the concept. An illustration is given in Figure 2.3.

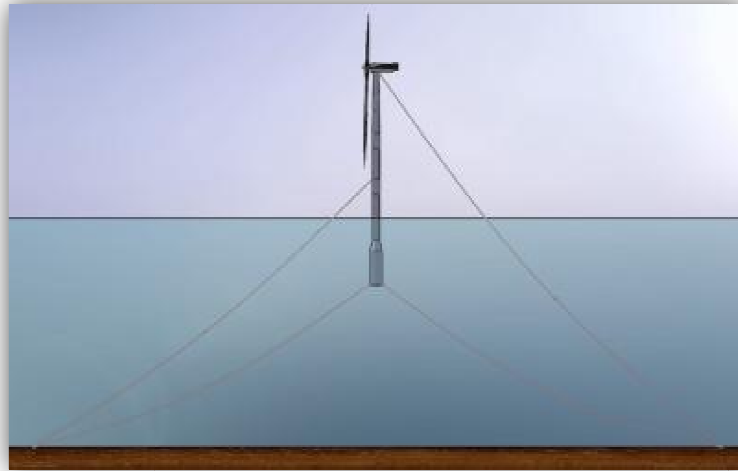


Figure 2.3 – Illustration photo of the Njord concept

2.3.4 WindSea

The WindSea concept is a semi-submersible with 3 corner columns. The floater supports 3 wind turbines, one on each corner column. Two of the rotors are of up-wind type and the third is of down-wind type, see Figure 2.4. Mooring lines are connected to a turret mechanism at the geometric center of the vessel. In a similar way as for the Sway system this should orient the turbines towards the wind. Extensive numerical calculations and model tests are performed. WindSea AS also plans to build a full-scale prototype of their concept (windsea.no).



Figure 2.4 – Illustration photo of the WindSea concept

2.3.5 WindFloat

The WindFloat concept is owned by Principle Power. It is not a Norwegian concept, but will be mentioned here as an interesting idea. The floater consists of three corner columns and the whole structure supports one windmill. As for most other concepts the platform is assumed to give good static stability. An advanced system is also proposed for better damping qualities. This is done by large area heave plates and an active ballasting system as illustrated on Figure 2.5. Extensive numerical modeling and experimental model-scale tests have been performed. Full-scale demonstrations are planned (principlepowerinc.com).



Figure 2.5 – Illustration photo of the WindFloat concept

2.4 Previous work

A lot of work has been done on the Hywind concept. Some of the most relevant work for this thesis is listed below.

In Nielsen et al. (2006a) and Nielsen et al. (2006b) two different simulation models are described and compared to the model scale experiments.

In Skaare et al. (2007) an advanced simulation tool was developed for simulation of the Hywind concept. This was done by combining the two independent programs HAWC2 and SIMO/RIFLEX. The results are compared to model scale experiments.

The Hywind floater has also been used as a basis for other published numerical studies:

In Jonkman et al. (2010) a model called the OC3-Hywind have been studied by the OC3 participants. The floater is similar to Hywind, however the mass distribution and the windmill is different. Specifications of the floater can be found in Jonkman (2009).

In Karimirad et al. (2009) a model similar as the Hywind concept is studied in extreme environmental condition.

2.4.1 Basic study on spar-buoys

As a preparatory study to this master thesis I studied the motion of free floating circular cylinders in waves, Linde (2009). This preparatory work will not be repeated here. Briefly explained the design philosophy behind deep draft floaters in general implies that the draft is adequately large to reduce first order heave excitation (Haslum 2000). For spar-buoys the vertical center of gravity (VCG) is often placed far below the center of buoyancy (VCB) to create good static stability.

3 NUMERICAL MODEL

As mentioned previously Marintek’s simulation software SIMO will be used for time simulations. The main objective has been to learn how a floating wind turbine can be modeled and analyzed using SIMO. In 2005 model scale experiments of Hywind were carried out at the Ocean Basin Laboratory at Marintek in Trondheim. This was a 5 MW version of the concept. I have access to some of these test results and will compare them with the numerical model. An illustration photo and main particulars of the concept are presented in Figure 3.1 and

Table 3.1. These data are taken from Nielsen et al. (2006a).



Figure 3.1 – Illustration photo of the Hywind concept

Turbine size	5 MW
Nacelle height above water line	81.5 m
Rotor diameter	123 m
Water depth	200 – 700 m
Displacement	7950 m ³
Mooring	3 lines

Table 3.1 – Main particulars of the 5 MW version of the Hywind concept

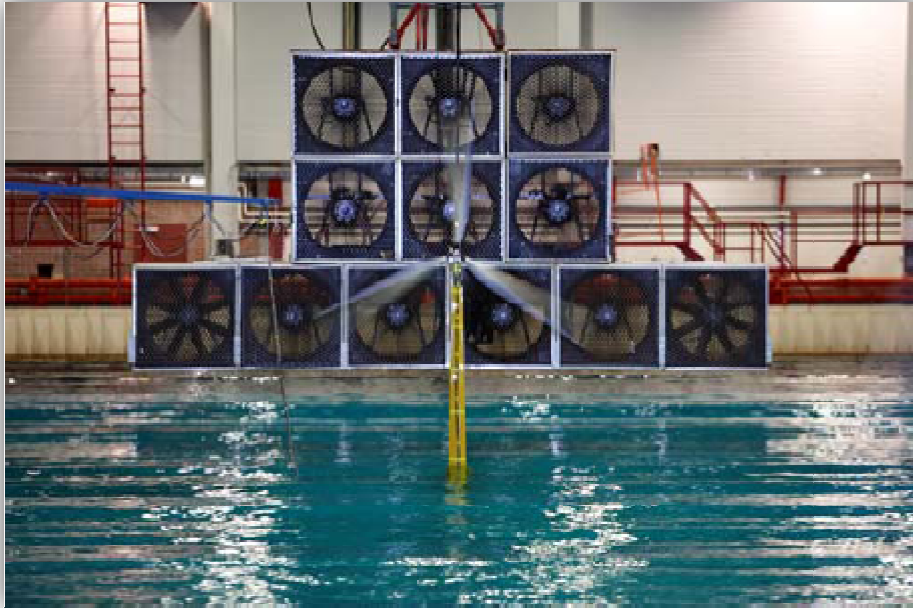


Figure 3.2 – Picture from the experimental model-scale test set-up

Most of the information I've been given about the software and especially the Hywind specifications are considered to be confidential. This information will not be presented in the main report, but are referred to the relevant documents. A list of the kind of information I had access to is given here:

- Geometry, mass and mooring line data for a floating 5 MW wind turbine concept of Hywind design, see Hanson (2008).
- A document describing the wind turbine analysis extension of SIMO, see Sintef (2009).
- Additional SIMO input files required for this wind turbine extension. Including a complete model similar to the OC3-Hywind described earlier. Results from previous studies on this wind turbine were also made available.
- The main report from the experimental model-scale test (Yttervik 2006).

3.1 Learning SIMO

Prior to modeling the Hywind structure I had to learn how the software works and how to use it properly. As it is a complex program I have spent a lot of time on this. Different existing

SIMO models were used and I attended some lectures about basic use of the software. The floater described in Hanson (2008) was built from scratch.

In order to learn how to use the wind turbine module in SIMO and to verify that it worked properly I started using the model provided by Marintek. I analyzed it for cases previously done by Marintek and compared the results. The results were the same.

3.2 Model specifications - uncertainties

In this section it will be referred to Hanson (2008) and Yttervik (2006) concerning some uncertainties about the specifications of the structure.

It must be mentioned that it has been difficult to interpret how the model actually was built. Looking at figure 1 and table 1 in Yttervik (2006) it seems to be some inconsistency with respect to the submerged volume. As the ‘cone section’ is somewhat different in the figure and the table this will result in two different submerged volumes and I do not know which version was used during the actual model test. Two different possibilities will be discussed:

1. Geometry no.1: First considering the ‘as built’ geometry given in the figure. Using this geometry will result in a submerged volume and vertical center of buoyancy-VCB as calculated in Appendix A. Then looking at the specified value of the weight of the structure including mooring. It is seen that this force from weight of the structure and mooring is not equal to the buoyancy force. It is also uncertain if the weight of the rotor is included in the specified total weight in table 1 from Yttervik (2006). If this is the correct geometry from the model tests this means that equilibrium at specified draught must be obtained by additional weight. Assuming the mooring system is specified correctly then its pretension is set. Then equilibrium must be obtained by extra weight compared to the ‘as built value’ specified in table 2 from Yttervik (2006). This could be weight from the rotor and equipment or additional weight for obtaining correct draught and trim. The total mass can be found from these assumptions, but the distribution of the mass is not known.
2. Geometry no.2: A second possibility is to consider the geometry as specified in table 1 from Yttervik (2006). The resulting submerged volume and VCB are calculated in

Appendix A. The resulting buoyancy force corresponds with the total weight of the structure with mooring as specified. Assuming this specified weight also includes the weight of the rotor it seems more likely that this is the correct geometry. However I do not know this for certain. This specified “full-scale” geometry and weight also corresponds to the specified model scale values assuming geometric similarity and Froude scaling. I also refer to pictures from the model test with waterline mark before and after final tuning of draught and trim, see Yttervik (2006). The pictures seem to be consistent with this second geometry version.

Numerical models of both geometry no.1 and no.2 were modeled as described in the following sections. Geometry no.2 was discovered very late in the project, but based on the discussion above I have chosen to present results from this geometry only. The correct mass distribution is still uncertain.

3.3 Linear and quadratic potential forces

The linear hydrodynamic problem in regular waves is solved using Det Norske Veritas’ (DnV’s) software Wadam, based on potential theory. This is done utilizing a three dimensional (3D) panel method. Potential theory and panel methods are well known and are described in literature, see e.g. Faltinsen (1990).

Wadam is a general analysis program for calculation of wave-structure interaction for fixed and floating structures of arbitrary shape, see DnV (2008). It is a part of DnV’s software package SESAM.

The panel mesh of the floater was modeled using DnV’s software GeniE. One quarter of the floater was modeled as it is symmetric about both the x-z and the y-z plane. This was done in order to reduce computational time and to be able to make a denser panel mesh (the Wadam version I had access to have a limitation of 3000 basic panels). In order to run Wadam without errors the mass force needs to be equal to the buoyancy force. Another option possible in Wadam is to balance the difference in buoyancy and mass with additional vertical pretension from “Morison anchor elements”. It should be mentioned that specifying the mass equal to the displaced mass in this particular case will not give the correct stiffness matrix and response amplitude operators (RAO’s) as calculated by Wadam. This is because of the nonlinear

contribution from mooring and will be discussed later. The excitation forces and frequency dependent added mass and damping will not be affected by this, these values only depend on the geometry of the submerged body. The panel mesh can be seen in Appendix A.

Similar calculations are presented in Jonkman (2009) for the OC3-Hywind geometry as mentioned earlier in this report. As done in Jonkman (2009) I chose to integrate the logarithmic singularity analytically, solve the linear system of equations using a direct solver, and remove the effects of irregular frequencies. The floater was analyzed at its undisplaced position (consistent with linear theory), and at a finite water depth (320m).

In this model I have also calculated mean drift forces in surge, sway (and yaw) using a conservation of momentum method. Mean drift forces in all six degrees of freedom could also be calculated by pressure integration. The results were a little bit different from the conservation of momentum method. One reason for this could be the density of the panel mesh. The results obtained from conservation of momentum were kept as this method is assumed to be less sensitive to the panel mesh. A second order surface mesh was also modeled in GeniE in order to calculate second order sum and difference frequency forces in Wadam. These calculations were however not used in the SIMO analysis.

3.3.1 Implementation in SIMO

As explained above the added mass and damping will have frequency dependence. This property is accounted for in the time domain by a convolution integral, where the so called retardation function is convoluted with previous values of the body velocity. The retardation function can be calculated from either the frequency dependent added mass or damping. The calculation of this linear memory effect is further described in SIMO (2009a) and Jonkman (2009).

Horizontal mean drift forces from the conservation of momentum calculations are implemented as drift force coefficients and written to the SIMO system description file. These coefficients will be used to obtain slow drift forces (difference frequency) in SIMO by a Newman model. For more information about this see SIMO (2009a).

The derivations of the mean drift and slow drift force expressions are quite extensive and it will be referred to text books, see for instance Faltinsen (1990).

I will not explain the Wadam results in detail as this discussion can be found in Jonkman (2009). However I will mention one important effect that can be seen from the heave excitation force, see Figure 3.3. It is seen that the force changes sign at an angular frequency around 0.25 rad/s. Then it increases to a peak around 0.5 rad/s before the magnitude drops again. This effect is called heave cancellation and it is well known for structures like semi-submersibles. Briefly one may say that the Froude-Kryloff force counteract the diffraction force. Spar buoys will normally not benefit from this effect as the Froude-Kryloff term is an order of magnitude larger than the diffraction term (Haslum 2000). Because of the stepped geometry near the surface the Hywind buoy can benefit from heave cancellation. See Haslum (2000) for more information about heave cancellation in the case of spar-buoys.

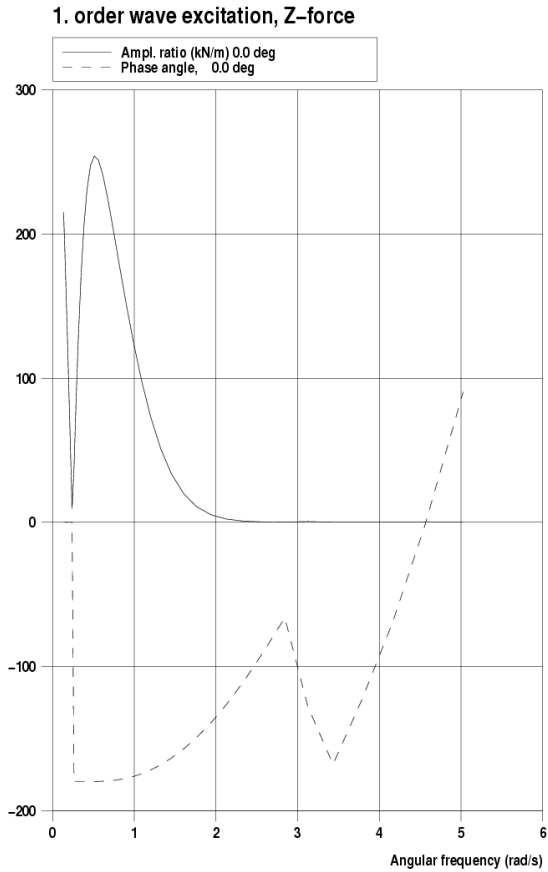


Figure 3.3 – Hydrodynamic-wave-excitation force in heave as calculated from Wadam

3.4 Damping

As a first approach to the problem I made a model similar to the one given to me by Marintek. The model given to me by Marintek is the same model as used in the OC3-Hywind comparison project, see Jonkman (2009). In this project they had access to the free decay time series from the experimental model test. The damping terms were adjusted so that the amplitudes from free decay in simulations approximately matched those from experiments. As discussed previously the OC3-Hywind model is not exactly the same as the one I have modeled. However as the structure is very similar I used the same damping contributions as a starting point.

All properties for the floater are specified in a body-coordinate system which in static equilibrium corresponds to the waterline. The model consists of a linear and a quadratic damping matrix:

$$B_{linear} = \begin{bmatrix} 100 \text{ kN}/(\frac{m}{s}) & 0 & 0 & 0 & 0 & 0 \\ 0 & 100 \text{ kN}/(\frac{m}{s}) & 0 & 0 & 0 & 0 \\ 0 & 0 & 130 \text{ kN}/(\frac{m}{s}) & 0 & 0 & 0 \\ 0 & 0 & 0 & 0 & 0 & 0 \\ 0 & 0 & 0 & 0 & 0 & 0 \\ 0 & 0 & 0 & 0 & 0 & 13000 \text{ kNm}/(\frac{m}{s}) \end{bmatrix} \quad (3.1)$$

$$B_{quadratic} = \begin{bmatrix} 0 & 0 & 0 & 0 & 0 & 0 \\ 0 & 0 & 0 & 0 & 0 & 0 \\ 0 & 0 & \frac{1}{8} \rho C_{D,bottom} \pi D_{bottom}^2 & 0 & 0 & 0 \\ 0 & 0 & 0 & 0 & 0 & 0 \\ 0 & 0 & 0 & 0 & 0 & 0 \\ 0 & 0 & 0 & 0 & 0 & 0 \end{bmatrix}$$

Where:

D_{bottom} is the diameter of the bottom of the cylinder.
 $C_{D,bottom}$ is the corresponding non-dimensional drag coefficient (set equal 1.0 as a first guess).

3.4.1 Quadratic drag forces

In order to account for viscous effects so-called distributed elements are added to the model in SIMO. The drag force on an element is calculated using the drag term from the Morison formula and may be written:

$$f_i = C_{q,i} U_{rel,i} |U_{rel,i}| \quad (3.2)$$

Where:

$C_{q,i}$ is the quadratic drag coefficient for element no. i given in full dimensions.

$U_{rel,i}$ is the relative velocity at the center of element no. i in the local element coordinate system.

The relative velocity may be written:

$$U_{rel,i} = \dot{X}_i - U_i - v_i \quad (3.3)$$

Where:

$v_i = [v_{ix} \ v_{iy} \ v_{iz}]^T$ is water particle velocity in local element coordinate system.

\dot{X}_i is element velocity in local element coordinate system.

$U_i = [U_{ix} \ U_{iy} \ U_{iz}]^T$ is current flow velocity in local element coordinate system.

The force on a single element acts at the center point of the element in the element coordinate system. This point force is added to the body. See SIMO (2009a) for more details on how this is implemented.

Horizontal drag forces are calculated using a strip theory model based on the cross-flow principle and relative velocity ‘‘Morison-elements’’. The spar buoy is divided into strips in the longitudinal direction. The force on each strip is given by equation (3.2). For a cylindrical shape the quadratic drag coefficient in full dimension is given by:

$$C_{q,i} = \frac{1}{2} \rho C_{D,i} D_i \Delta Z_i \quad (3.3)$$

Where:

- ρ is the density of the fluid = 1025kg/m³.
- D_i is the diameter of the strip/cylinder.
- $C_{D,i}$ is the non-dimensional horizontal drag coefficient for element no. i .
- ΔZ_i is the height of element no. i .

The distributed element model was adjusted to fit the new geometry and the number of strips was increased. The number of drag elements/strips is assumed to be sufficiently high. This was also seen by performing a sensitivity check in SIMO. This is important in order to capture the dynamics of the relative velocity.

The drag coefficient C_D will depend on several parameter like the Kaulegan-Carpenter number - KC , Reynolds number - Re and a roughness number k/D . Experimental values of C_D can be found in e.g. Sarpkaya (2010). $C_D = 0.6$ is used in the model given by Marintek. This is a typical value for large Re .

Drag elements may also be specified at body fixed points in order to account for other viscous effects. This was not done in the first approach to the problem.

3.5 Restoring forces and moments

When a body is freely floating, the restoring forces will follow from hydrostatic and mass considerations, se e.g. Faltinsen (1990).

3.5.1 Linear stiffness matrix

The contributions from hydrostatic and mass considerations are included in a linear stiffness matrix for the floating body in SIMO. The spar-buoy has both the x-z and y-z plane as a symmetry plane for the submerged volume. The only non-zero coefficients are:

$$\begin{aligned} C_{33} &= \rho g A_{WP} \\ C_{44} = C_{55} &= \rho g V z_B + \rho g S_{WP} - M g z_G \end{aligned} \quad (3.4)$$

Where:

$A_{WP} = \frac{1}{4}\pi D_{WP}^2$ is the waterplane area. D_{WP} is the cylinder diameter at the water plane

$S_{WP} = \frac{1}{64}\pi D_{WP}^4$ is the water plane stiffness

M is the structural mass

V is the displaced volume of the spar-buoy

z_B is the vertical center of buoyancy

z_G is the vertical center of gravity

In SIMO the floater is modeled as a rigid body without the option ‘GRAVITY INCLUDED’. This means that the restoring force from mass is not included automatically by the computer code. Consequently the restoring from mass must be included in the linear stiffness matrix as described above. Another possibility would be to include the option ‘GRAVITY INCLUDED’ and only include hydrostatic contributions in the linear stiffness matrix.

3.5.2 Mooring lines

For a moored structure additional restoring forces are added to the hydrostatic and mass contributions (Faltinsen 1990).

The specifications of the Hywind mooring system can be seen in Hanson (2008). The system consists of three mooring lines. Each mooring line is attached to the spar at two fairlead points with a so-called ‘crowfoot’ or delta-lines. In addition the lines also include clump weight. An illustration of the mooring can also be seen in Figure 3.1.

Implemented in the SIMO system there is a possibility to model mooring lines as catenaries. This is based on the mooring analysis program MIMOSA , see SIMO (2009a) and SIMO (2009b). I have modeled the mooring lines with the different segment properties specified for the Hywind system, however with some simplifications. The problem is solved in two dimensions (2D) in SIMO and consequently each mooring line is attached to the spar-buoy at only one fairlead, neglecting the effect of the “crowfoot”. The mooring lines are attached to the spar-buoy at fairleads as seen in figure, Figure 3.4. The two delta lines are modeled as one segment in the 2D mooring line. This segment has the same properties as one individual delta line except for double weight and stiffness. The other segments of the line are modeled as

specified for the real system, including a clump weight. The analysis used is quasi static and damping caused by drag on the lines is not accounted for.

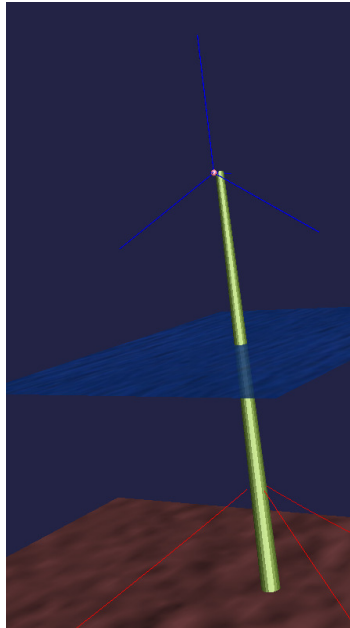


Figure 3.4 – Illustration photo from the numerical simulations

Pretension and geometrical shape are considered to be important parameters. I have moved the anchors in the horizontal plane in order to get the correct pretension as specified in Yttervik (2006). The geometrical shape is also assumed to be very similar as for the specified system. In order to keep the spar-buoy at the correct draught in static equilibrium a specified force is defined at the body origin pointing upwards. This constant force is equal in magnitude as the initial pretension. In this way the restoring moments in pitch and roll caused by the pretension are accounted for. See Sintef (2009) for more details about this specified force.

The effect from the ‘crowfoot’ is simplified by a linear stiffness in yaw and added to the linear stiffness matrix specified for the floater.

$$C_{66} = 98\,340 \text{ kNm/rad} \quad (3.5)$$

I have used the same value as for the OC3-Hywind model. In the simplest model presented in Nielsen et al. (2006a) the same approach is used. They approximated the yaw stiffness by the moments due to the mooring forces at the connection point of the “crowfoot”. This simplified model will not properly account for possible nonlinear behavior of the “crowfoot”.

The restoring characteristics for surge motion will be different in the positive and negative direction because the mooring system is not symmetric about the y-z plane. The static restoring characteristics for the positive surge motion are compared with results from the model test, see Yttervik (2006). The results from SIMO are very similar as the experimental test results.

An attempt was made to include the delta lines in the mooring system. Except for the delta lines the rest of the mooring line was modeled as described above. The mooring line was connected to a body in SIMO. This body was used as a connection node and two line couplings connected this body to the spar-buoy. Some time was spent on this modeling, but the problem was finally simplified as described above. The anchor system could also be modeled in RIFLEX and include delta lines and other dynamic effects. Then drag on the lines could also be included. However this was not done in this project.

3.6 Mass properties/matrix

The mass coefficients of the floater are transformed to the coordinate system used in SIMO. This is a body related coordinate system with origin at the initial mean free surface. See APPENDIX A for mass calculations.

3.7 Modeling the rotor module

3.7.1 Rotor

As I didn't have the correct data for the rotor I used the rotor from the model given to me by Marintek. The rotor blades used in the BEM model are from the 5MW NREL turbine used in the OC3-Hywind project, see Jonkman (2009). More information about the BEM code can be found in Sintef (2009). The BEM code should be able to model the rotor blades used in the model test if the coefficients for the NACA44XX profile were given. The mass distribution of the rotor (hub+blades+shaft) used in the model test should also be known. This information is not available and instead I will use the known 5MW NREL turbine, with some modifications. It is thereby stated that this is not the same rotor as used in the Hywind model test.

3.7.1.1 Couplings

The rotor is coupled to the support structure as described in Sintef (2009). The vertical position of the rotor and couplings to support structure is changed according to a nacelle height of 81.5m. It is also possible to do further changes on the position of the rotor and the angle of rotation axis.

3.7.2 Tower

In order to include drag forces from the tower I simply used the drag coefficients from the available Marintek model. The input for wind area of the tower was reduced. This was done approximately according to the difference in size of the tower used in the Marintek model and the tower specified for Hywind.

3.7.3 Nacelle

In some simulations an additional body was connected to the support structure at the nacelle height specified in Table 3.1. The weight of this body was set very small so that it wouldn't affect any results. The reason for including this body was to get quick estimates of the motion at nacelle level during simulations.

4 COMPARISON OF NUMERICAL MODEL WITH EXPERIMENTAL MODEL TEST RESULTS

4.1 The different test conditions

The different test conditions for which results are compared are listed in

Table 4.1. The waves are based on a JONSWAP spectrum and the wind is based on an NPD spectrum.

Test number:	Hs [m]	Tp [s]	Windspeed [m/s]	Control strategy
1	5	12	0	A0
2	9	13	0	A0
3	14	15	0	A0
4	-	-	17	AN
5	5	12	17	AN
6	5	12	17	B

Control strategy:
A0 = No wind, rotor blade is fixed.
AN = Constant rotational speed, constant pitch.
B = Conventional wind turbine control, without active damping.

Table 4.1 – Specification of test conditions

4.2 Comparison procedure

In order to validate numerical calculations by model test results there are many aspects to consider. The procedure will vary between different concepts and tests (Aarsnes 2008). An example of a validation procedure is given in Aarsnes et al. (2008). This example is used in the following to explain important steps in the comparison of my numerical calculations and the experimental tests:

1. Equal model loading conditions:

The following parameters should be the same in the model tests and numerical calculations:

4 COMPARISON OF NUMERICAL MODEL WITH EXPERIMENTAL MODEL TEST RESULTS

- Geometry: This parameter is uncertain as discussed previously. If the geometry is incorrect it will affect many parameters. The two geometries discussed previously are very similar. It is assumed that the response also will be similar. The rotor is not the same in the model test and the numerical model.
- Draft and trim of the spar-buoy: The initial draft is the same as in the model test. The trim is set to zero degrees in the numerical model and it is assumed that this also was the case during the model testing. For the test conditions including wind the spar has a slight forward trim in the numerical code.
- Metacentric height (GM_T and GM_L): This parameter is also uncertain, but it is assumed to be approximately the same. Difference in metacentric height will have a large effect on the results.
- Radius of gyration r_{xx} , r_{yy} and r_{zz} : This parameter is probably not correct, but it is assumed to be similar. The radius of gyration of the rotor (hub, blades and shaft) are not known.
- Mooring system: due to dynamic effects the line tension in experiments may deviate from the tension predicted by the quasi static analysis. The mooring systems main intention is to counteract mean environmental forces. Less horizontal stiffness should cause a larger mean horizontal response. This is tested by moving the anchors towards the spar to give less horizontal stiffness. The results were a larger mean value. However the restoring characteristics in surge seem to be very similar as for the model test, see Yttervik (2006). As the mooring system is not symmetric it is important that the anchors are placed at the same positions as in the experimental test set-up. If the anchor positions are not the same the mean values could become different.

2. Equal environmental data:

Waves

- For irregular waves parameters like H_s , T_p and spectral shape should be the same. I have modeled the environment in three different ways. First a JONSWAP specter was applied in SIMO using the specified values for H_s , T_p and γ . As a second approach a JONSWAP specter was modeled using the parameters obtained from the actual model tests, see Yttervik (2006). As a third option I used the calibrated wave signal from the model basin as direct input to SIMO. It is possible to obtain similar wave conditions,

4 COMPARISON OF NUMERICAL MODEL WITH EXPERIMENTAL MODEL TEST RESULTS

but the spectrum should be compared with the spectrum from the model test to ensure this. It was seen that difference in the irregular wave spectrum can have a large effect on the results.

- In the numerical calculations the spar-buoy was analyzed at the same finite water depth (320m) as in the experimental tests.

Wind

Similar as for irregular waves I have modeled the wind conditions in two different ways in SIMO. The wind can be specified using the ISO 19901-1 (NPD) spectrum with specified wind velocity, see (SIMO 2009a). Also for wind time series SIMO can read calibrated data from the actual model test.

Using Fast Fourier Transform (FFT)

In most of my calculations I have used the Fast Fourier Transform (FFT) for generation of time series or the wave time series from the model test have been used directly. An important limitation present in both these methods is that the wave kinematics is described at one specified position before the simulation starts. In SIMO I also generated waves by cosine series in the time domain. This makes it possible to evaluate the wave kinematics at the spar-buoy's actual displaced position. The inconvenience is that the method is very time consuming. It was seen that the results were slightly different by comparing the results from the cosine series approach and the FFT.

3. Equal test conditions:

- Wave heading and wind direction: are the same (0 degrees).
- Transient effects: both the model test result and the results from SIMO contain transients. This is handled by removing the first part of the results that contain transients.

4. Natural periods:

I did not have access to the free decay time series from the experimental tests. However I performed free decay tests in SIMO. The natural periods obtained from

SIMO were very similar as the natural periods obtained from the experimental tests. The damping contributions are uncertain.

5. Comparison of results:

It would be preferable to compare response results in regular waves as a first check. However this is not available.

The test conditions may contain both irregular waves and gusty wind. The simulations will contain both WF and LF responses. In the following comparison of experimental and numerical results I will only show mean values and standard deviation. This is done by request from Statoil because of confidentiality. From this simple comparison the standard deviation is considered the most important parameter. The standard deviation gives an indication of the averaged amplitudes.

Because of all the uncertainties regarding how the experimental model was built it is quite difficult to state the reason for any difference between numerical and experimental results. Some possible improvements will be discussed.

4.3 Test number 1,2 and 3 – without wind

The modeling procedure described previously was first used to make a 1-body model in SIMO. By 1-body I mean a model of the whole structure as one rigid body without any other bodies connected to it. I have used the ‘specified’ value for the total mass of the structure assuming that this also includes the mass of the rotor when it is fixed from rotating. The additional rotor body with BEM code and corresponding couplings, see Sintef (2009), are not included.

Results obtained from SIMO are compared to results from the experimental tests in Table 4.2. It can be seen that the standard deviations are similar, but are in general underestimated by the numerical calculations. A possible reason for the difference in mean horizontal position of the buoy could be the mooring system. As mentioned previously the horizontal mooring stiffness will affect the mean horizontal position.

4 COMPARISON OF NUMERICAL MODEL WITH EXPERIMENTAL MODEL TEST RESULTS

		Standard deviation		Mean value	
		SIMO result	Experimental result	SIMO result	Experimental result
Test condition no.1	XG_Nacelle	1,45461	1,51802	0,08040	0,15677
Hs = 5m	Pitch	0,43827	0,48344	0,00903	-0,01688
Tp = 12s	ZG_Global	0,15062	0,17319	0,00016	-0,22455
No wind	XG_Global	0,83444	0,86664	0,06755	0,18117
Rotor is fixed from rotating.					
Test condition no.2	XG_Nacelle	3,01053	3,27553	0,11936	0,12926
Hs = 9m	Pitch	0,89875	1,00149	0,01367	-0,03858
Tp = 13s	ZG_Global	0,33022	0,38308	-0,00024	-0,25743
No wind	XG_Global	1,73784	1,96476	0,09991	0,18507
Rotor is fixed from rotating.					
Test condition no.3	XG_Nacelle	6,03188	6,54838	0,22563	0,51627
Hs = 14m	Pitch	1,77657	1,99907	0,02438	-0,00826
Tp = 15s	ZG_Global	0,69427	0,76414	-0,00435	-0,24846
No wind	XG_Global	3,51813	3,89961	0,19094	0,52892
Rotor is fixed from rotating.					

Table 4.2 - Comparison of some results from test condition 1, 2 and 3. Drag forces evaluated up to mean surface.

Where:

XG_Nacelle is the position of the nacelle in x-direction in the Global SIMO system.

XG_Global is the position of the buoy in x-direction in the Global SIMO system. The body fixed point that coincides with the free surface at in initial position.

ZG_Global is the position of the buoy in z-direction in the Global SIMO system. The body fixed point that coincides with the free surface at in initial position.

Pitch is the pitch angle of the buoy (in degrees), given in a local body coordinate system. Positive direction when top end moves away from the environment direction in this case.

The Global SIMO coordinate system is fixed at the free surface at the initial position of the buoy. Positive x-direction away from the environment direction in this case. Positive z-direction upwards.

4.3.1 Possible improvements

4.3.1.1 Fixed drag elements

Because of the long draft of the spar-buoy it could be that the use of a quadratic damping matrix in heave don't give a good enough impression. It is assumed that viscous drag on the bottom of the spar will cause much of the quadratic damping. This viscous drag will then have a large moment arm because of the long draft. One possibility is to place a fixed drag element at the bottom of the spar instead of in a quadratic matrix for the body.

The drag force on this fixed element could then be described by equation (3.2).

Where:

$$C_{q,bottom} = \frac{1}{8} \rho C_{D,bottom} \pi D_{bottom}^2 \quad (4.1)$$

it is here assumed that the drag force is proportional to the area of the bottom of the spar.

It could further be assumed that viscous drag will appear where we see a change in the geometry, see the step/ cone section in Figure 3.1. A drag element could also be placed there. Both of these assumptions were studied in SIMO, but the difference in results was quite small.

Another contribution to damping is the mooring system. This is also assumed to be of quadratic behavior. As explained previously the mooring analysis in the numerical calculations do not account for this damping. Consequently this damping contribution must be added in matrix form or by Morison drag elements.

In SIMO I checked the sensitivity to changing the horizontal drag coefficient for the strip model. The drag is assumed to be of much greater importance for the low frequency (LF) motions than for the wave frequency (WF) motion. Looking at the surge motion it was seen that the mean value and standard deviation were not sensitive to a small change in drag coefficient, the maximum and minimum values were however very sensitive. From spectral analysis in SIMO it seems like the peaks for LF horizontal motions are underestimated when using $C_D = 0.6$. This could be an indication of wrong damping.

4 COMPARISON OF NUMERICAL MODEL WITH EXPERIMENTAL MODEL TEST RESULTS

4.3.1.2 Viscous drift

Using the same model as above I also made an attempt to include viscous drift forces. This was done by using the same strip model describing distributed drag forces. Instead of evaluating the drag forces up to the mean free surface I chose to evaluate them up to the instantaneous free surface. This method should be used with care, but it will here be used in order to illustrate a possible viscous contribution. The importance of viscous effects should also increase with increasing wave amplitude, see Faltinsen (1990). Results from these simulations can be seen in Table 4.3.

		Standard deviation		Mean value	
		SIMO result	Experimental result	SIMO result	Experimental result
Test condition no.1	XG_Nacelle	1,45816	1,51802	0,10754	0,15677
Hs = 5m	Pitch	0,43917	0,48344	0,01203	-0,01688
Tp = 12s	ZG_Global	0,15062	0,17319	0,00016	-0,22455
No wind	XG_Global	0,83814	0,86664	0,09042	0,18117
Rotor is fixed from rotating.					
Test condition no.2	XG_Nacelle	3,01744	3,27553	0,18355	0,12926
Hs = 9m	Pitch	0,90067	1,00149	0,02070	-0,03858
Tp = 13s	ZG_Global	0,33023	0,38308	-0,00032	-0,25743
No wind	XG_Global	1,74475	1,96476	0,15411	0,18507
Rotor is fixed from rotating.					
Test condition no.3	XG_Nacelle	6,03926	6,54838	0,31927	0,51627
Hs = 14m	Pitch	1,77924	1,99907	0,03437	-0,00826
Tp = 15s	ZG_Global	0,69447	0,76414	-0,00466	-0,24846
No wind	XG_Global	3,52490	3,89961	0,27038	0,52892
Rotor is fixed from rotating.					

Table 4.3 - Comparison of some results from test condition 1, 2 and 3. Drag forces evaluated up to instantaneous surface.

4.4 Test number 4, 5 and 6 – including wind

For the results presented here I have used a 2-body model in SIMO. The spar-buoy is modeled as in the previous tests, but I have used a different mass when calculating the linear stiffness matrix and the mass distribution. The mass distribution used for the spar is approximately the

4 COMPARISON OF NUMERICAL MODEL WITH EXPERIMENTAL MODEL TEST RESULTS

same as the “as built” values given in (Hanson 2008). In addition the 5 MW NREL turbine is coupled to the spar-buoy as described in chapter 3. The mass of the turbine is 110 ton, giving the floater a slight forward trim. The trim could be adjusted by additional weight, but this is not done.

In the previous tests slow drift from waves was present. In the case of a floating wind turbine slow drift will be caused by wave drift, wind on the tower and rotor and possible contributions caused by the control strategy used.

I have not used time on fine tuning the turbine in the numerical code with the turbine from the experimental model scale tests. This is both because of lack of input data and because the hydrodynamic part is considered the most important in this thesis.

It was seen that the thrust from the rotor in the numerical code was initially much larger than in the experimental test results. There could be several reasons for this. Firstly the wind turbine module is different. Both are 5MW turbines, but the diameter of the 5MW NREL rotor is 126m and the rotor from the experiments is specified to 123m full-scale. The wing profile and the weight are different and the control system is not the same. Another important factor is that the thrust in model-scale experiments could be significantly lower than what is specified for full-scale because of scale effects.

The fact that the control systems are not the same made the simulations difficult. The wind turbine module I had access to for SIMO use a conventional control strategy, see Sintef (2009). The strategy is based on the measured electrical torque and the rotation velocity. The control algorithm used in the experiments is based on measured thrust and relative wind velocity, see Nielsen (2006a) for more information. Otherwise the two control strategies are similar. The main idea is to obtain maximum power below a rated value. Above this rated value the idea is to keep the power constant by controlling the pitch angle of the rotor blades.

I first used the default values of the conventional control algorithm I had available. These default values are given as an example in Sintef (2009). To get the thrust more similar to the experiments I lowered the value for rated and maximum electrical torque. In this way the

4 COMPARISON OF NUMERICAL MODEL WITH EXPERIMENTAL MODEL TEST RESULTS

thrust force became similar as in the experiments. It is possible to tune these values to fit even better to the experimental values.

It was said that test no.4 and no.5 had a constant rotor speed and a fixed blade pitch angle. This caused some troubles as it is normal to have either fixed blade pitch (below a rated power) or constant power output (above a rated power). In the numerical code I used a constant blade pitch angle for these two tests. The rotation speed is consequently not constant. As for the conventional control strategy I only tuned the numerical code approximately similar as the one from experiments. I used the same fixed blade angle as specified in Yttervik (2006). This control strategy could also be tuned better. It is assumed that using the same fixed blade pitch for two different blade profiles will not give exactly the same thrust. Results from tests including wind are compared in Table 4.4.

		Standard deviation		Mean value	
		SIMO result	Experimental result	SIMO result	Experimental result
Test condition no.4	XG_Nacelle	2,50795	1,90600	13,14509	15,61452
No waves	Pitch	0,86559	0,40822	2,04464	2,62893
-	ZG_Global	0,12064	0,08888	-0,15767	-0,32303
Wind = 17m/s	XG_Global	1,59162	1,55670	10,23670	11,87960
Rotor blade pitch control strategy = rotor blade pitch is fixed.					
Test condition no.5	XG_Nacelle	2,70928	2,36200	13,17762	16,08265
Hs = 5m	Pitch	0,91671	0,61942	2,04539	2,70124
Tp = 12s	ZG_Global	0,18762	0,18820	-0,15796	-0,22447
Wind = 17m/s	XG_Global	1,67869	1,71542	10,26817	12,24434
Rotor blade pitch control strategy = rotor blade pitch is fixed.					
Test condition no.6	XG_Nacelle	1,99143	1,55770	16,63154	17,77491
Hs = 5m	Pitch	0,67688	0,49540	2,64388	2,99197
Tp = 12s	ZG_Global	0,25622	0,19647	-0,23523	-0,36070
Wind = 17m/s	XG_Global	1,09465	0,91429	12,87077	13,52352
Rotor blade pitch control strategy = conventional rotor blade pitch control.					

Table 4.4 - Comparison of some results from test condition 4, 5 and 6. Drag forces evaluated up to mean surface.

It is seen that the results obtained from numerical simulations and the experimental test results are not exactly the same. This is natural as the input values in the numerical calculations are

4 COMPARISON OF NUMERICAL MODEL WITH EXPERIMENTAL MODEL TEST RESULTS

assumed to be different from the values used in the experiments. The results given in Table 4.4 are however similar to the experimental test results, considering the uncertainties mentioned previously. This is as an indication that the numerical model used in SIMO may be able to give realistic results. However the input quantities should be known and better tuning of the turbine should be performed before stating a conclusion. The standard deviation from test no.5 (fixed blade pitch) in general seems to be larger than for test no.6 (conventional pitch control). This is the case for both numerical and experimental results. Prior to the experimental model tests it was assumed that the conventional blade pitch control could cause a negative damping contribution. In the tests I have studied in this thesis the conventional control strategy seems to give better response characteristics than for constant blade pitch.

5 CONCLUSION

The numerical model established in SIMO shows similar results compared to experimental model-scale test results. However the numerical results obtained are far from perfect. Because of uncertainties regarding how the experimental model was built it has been difficult to state a reason for any difference between numerical and experimental results. The concept specifications should be known more precisely and better tuning of the turbine should be performed before stating a conclusion on how the numerical tool performs.

6 RECOMMENDATIONS FOR FURTHER WORK

In further work I would contact Statoil and ask them more specifically about how the model actually was built during experimental testing. If these data are made available the numerical model presented in this thesis could be validated with the experimental test results.

Using this already established numerical model from SIMO it would be interesting to also include RIFLEX in the analysis.

It would also be interesting to compare the simulation program with full-scale results from Hywind when these results are available.

Confidential material is not published, but will be given to my supervisor, Professor Bjørnar Pettersen, in case some students will do further work on this subject. This includes Appendix A and some input files for SIMO.

7 REFERENCES

- Aarsnes, J. V. (2008). *Experimental methods in marine hydrodynamics*. Trondheim, Marinteknisk senter.
- Cordle, A. (2010). *State-of-the-art in design tools for floating offshore wind turbines*. Deliverable D4.3.5 (WP4: Offshore Foundations and Support Structures).
- DNV (2008). *Sesam user manual. Wadam. Wave Analysis by Diffraction and Morison Theory*: 210.
- Faltinsen, O. M. (1990). *Sea loads on ships and offshore structures*. Cambridge, Cambridge University Press.
- Fylling, I. (2010). *Floating wind turbine. Wave induced motions and loads*. Wind Power R&D seminar - deep sea offshore wind, Trondheim, Norway.
- Hanson, T. D. (2008). *Typical geometry and mooring line data for a floating 5 MW wind turbine concept of Hywind design*. F. G. Nielsen, StatoilHydro.
- Haslum, H. A. (2000). *Simplified methods applied to nonlinear motion of spar platforms*. Trondheim, NTH. 2000:101: XII, 139, 132 s.
- Jonkman, J. (2009). *Definition of the Floating System for Phase IV of OC3*, National Wind Technology Center (NWTC) and National Renewable Energy Laboratory (NREL).
- Jonkman, J., Larsen, T., Hansen, A., Staerdahl, J. W., Fylling, I., Karimirad, M., Gao, Z., Moan, T., Nygaard, T., Maus, K., Nichols, J., Kohlmeier, M., Kossel, T., Zielke, W., Vergara, J. P., Merino, D. and Armendariz, J. A. (2010). *Offshore Code Comparison Collaboration within IEA Wind Task 23: Phase IV Results Regarding Floating Wind Turbine Modeling*. 2010 European Wind Energy Conference (EWEC), Warsaw, Poland.
- Karimirad, M., Gao, Z. & Moan, T. (2009). *Dynamic Motion Analysis of Catenary Moored Spar Wind Turbine in Extreme Environmental Condition*. European Offshore Wind Conference 2009. Sweden: 10.
- Linde, B. (2009). *Motion of a Circular Cylinder in Waves*. Trondheim, NTNU.
- Nielsen, F. G., Hanson, T. D. and Skaare, B. (2006a). *Integrated Dynamic Analysis of Floating Offshore Wind Turbines*. 25th International Conference on Offshore Mechanics and Arctic Engineering, Hamburg, Germany, ASME.
- Nielsen, F. G., Hanson, T. D. and Skaare, B. (2006b). *Integrated Dynamic Analysis of Floating Offshore Wind Turbines*.
- Nilsen, J. (2010). *Vil konkurrere ut Hywind*. Teknisk Ukeblad. Norway, Teknisk Ukeblad Media AS: 86.

7 REFERENCES

norwind.no. (2009). "*Alpha Ventus.*" Retrieved 4 May 2010, from <http://www.norwind.no/en/News/091001_AlphaVentus.aspx>.

principlepowerinc.com. "*Windfloat.*" Retrieved 20 May, 2010, from <<http://www.principlepowerinc.com/products/windfloat.html>>.

Sarpkaya, T. (2010). *Wave forces on offshore structures*. Cambridge, Cambridge University Press.

SIMO, p. t. (2009a). *SIMO - Theory Manual Version 3.7*. Marintek Report. Trondheim, SINTEF: 124.

SIMO, p. t. (2009b). *SIMO - User's Manual Version 3.7*. Marintek Report. Trondheim, SINTEF: 38.

Sintef (2009). *Floating wind turbines simulation. Rigid-body simulation by use of SIMO with extension.*

Skaare, B., Hanson, T. D., Nielsen, F. G., Yttervik, R., Hansen, A. M., and K. Thomsen, Larsen, T. J. (2007). *Integrated Dynamic Analysis of Floating Offshore Wind Turbines*. EWEC.

Statoil.com. "*Sway and ChapDrive.*" Retrieved 2 May, 2010, from <<http://www.statoil.com/en/TechnologyInnovation/NewEnergy/RenewablePowerProduction/Offshore/Pages/SwayChapDrive.aspx>>.

Statoil.com. (2008, 21 Jan). "*Dogger Bank; Awarded wind contract for Dogger Bank.*" Retrieved 4 May, 2010, from <<http://www.statoil.com/en/TechnologyInnovation/NewEnergy/RenewablePowerProduction/Offshore/DoggerBank1/Pages/DoggerBank.aspx>>.

Statoil.com. (2009, 10 Dec 2009). "*Hywind: Putting wind power to the test.*" Retrieved 4 May, 2010, from <http://www.statoil.com/en/technologyinnovation/newenergy/renewablepowerproduction/ons_hore/pages/karmoy.aspx>.

Statoil.com. (2009, 16 Jun 2010). "*Sheringham Shoal; Off the UK coast, we're planning a major new source of sustainable energy.*" Retrieved 20 June, 2010, from <<http://www.statoil.com/en/TechnologyInnovation/NewEnergy/RenewablePowerProduction/Offshore/SheringhamShoel/Pages/default.aspx>>.

sway.no. "*Principles of the Sway System.*" Retrieved 25 March, 2010, from <<http://sway.no/?page=166&show=177>>.

windsea.no. "About Windsea. An introduction." Retrieved 25 March, 2010, from <<http://www.windsea.no/about-windsea/>>.

www.ieawind.org. "*Subtask 2: Research for Deeper Waters. Offshore Code Comparison Collaboration (OC3).*" Retrieved 17 May, 2010, from <<http://www.ieawind.org/Annex%20XXIII/Subtask2.html>>.

Yttervik, R. (2006). *Model test of offshore floating wind turbine*. Trondheim, Norsk Hydro Produksjon AS: 153.